A Novel Methodology for Determining Steady-State Security Regions Using Artificial Neural Networks in Near Real-Time Applications

Guilherme de O. Alves, and João A. Passos Filho, *Senior Member, IEEE*

***Abstract*—The increasing penetration of variable renewable energy sources, such as photovoltaic and wind power, poses significant challenges to the real-time security assessment of power systems. In this context, the Steady-State Security Regions framework has emerged as a robust tool for voltage security assessment, providing valuable insights into the steady-state operating limits of electrical networks. However, the computational burden associated with determining these regions during system operation remains a major obstacle for current methodologies. This paper presents a novel approach for efficiently identifying these regions using artificial neural networks, enabling the fast and accurate delineation of security boundaries suitable for real-time and near-real-time applications. The methodology was validated on the IEEE 9-Bus and New England test systems, achieving accuracy comparable to conventional techniques while reducing computational time by up to 96%. The results underscore the potential of the proposed method as a scalable and effective tool to support operational decision-making in power systems with high shares of renewable generation.**

Link to graphical and video abstracts, and to code: https://latamt.ieeer9.org/index.php/transactions/article/view/9807

***Index Terms*—Artificial neural networks, power system operation, security assessment, steady-state security regions.**

I. Introduction

POWER systems have been experiencing a series of paradigm shifts in recent years, primarily driven by climate change. The increasing integration of non-dispatchable generation sources, such as solar and wind power, and the presence of distributed generation in electrical grids are the main factors behind these significant operational and planning challenges.

Additionally, the introduction of energy storage systems and demand response strategies is expected to drive even more substantial changes in the coming years. The current electrical infrastructure may not be prepared to manage the decentralized and intermittent nature of these resources, which can lead to issues related to reliability and stability, including voltage and frequency fluctuations. Moreover, there are challenges associated with operation, planning, and network sizing [1].

In this context, various computational methodologies have been developed to address the increasing complexity of power system operation. Among these, Dynamic Security Assessment (DSA) and Voltage Security Assessment (VSA) are widely used to evaluate whether a power system satisfies established reliability and security criteria. VSA focuses on assessing system performance under steady-state conditions, while DSA evaluates the dynamic response of the system to disturbances such as faults or abrupt load variations [2]–[7]. Both methodologies involve analyzing a base (reference) operating point and a predefined set of contingencies. The results are commonly presented using nomograms, which are two-dimensional graphical tools that depict security margins across key variables, thereby supporting operational decision-making.

The Steady-State Security Region (SSR) is a powerful VSA tool developed to provide insight into the steady-state operating conditions of a power system. It is represented by a three-dimensional surface that visualizes the secure operating region of the system, considering a division into three generation groups. This secure region is enclosed by a boundary that marks the onset of violations of steady-state security limits. These limits include, for example, voltage constraints at buses, reactive power limits of generators, and MVA limits of transmission lines and transformers, among others.

Reference [6] presents the state of the art for assessing power security in real-time, rather than offline simulations. The book is primarily geared toward the practical aspects of the subject, considering transmission systems. Several approaches to solving the VSA/DSA problem around the world are presented. On the other hand, references [8], [9] discuss methodologies for applying Steady-State Security Regions in distribution systems. Reference [8] presents an effective evaluation of the operating conditions of distribution systems with high penetration of Distributed Energy Resources, focusing on the intermittence of the new generation resources. The paper [9] addresses the geometric properties of the Distribution System Security Region, analyzing its shape and size by defining geometric indices using Monte Carlo sampling. This approach can be computationally expensive, particularly for high-dimensional systems.

The analysis of SSR [2]–[4], [6], [7], associate with VSA approach, in power systems is crucial for ensuring the security and reliability of electricity supply. SSR analysis involves

The associate editor coordinating the review of this manuscript and approving it for publication was Giner Alor-Hernández (*Corresponding author: Guilherme Alves*).

Guilherme Alves is with Department of Electrical Engineering, Federal Center for Technological Education "Celso Suckow da Fonseca", Rio de Janeiro, Brazil (e-mail: guilherme.alves@cefet-rj.br).

J. A. P. Filho is with Department of Electrical Energy, Federal University of Juiz de Fora, Minas Gerais, Brazil (e-mail: joao.passos@ufjf.br).

determining secure operational points, evaluated by criteria, enabling the identification and mitigation of failure and disturbance risks [4], [10]. However, constructing these regions requires numerous power flow solutions, leading to significant computational costs [2], [11].

Initial SSR studies employed linearized power flow to examine the security region [10], [12], [13]. This approach resulted in a substantial reduction in computational effort and offered reasonable accuracy, which varied according to the system's characteristics. However, in systems operating at boundary operating points, this accuracy tends to decrease. Over the years, methods have been developed to determine the SSR using the decoupled method for power flow analysis [14], [15], which is less computationally costly when compared to the Full Newton-Raphson method. However, the decoupled method may encounter numerical efficiency issues as it disregards the relationship between active power and voltage at the system's buses.

Subsequently, formulations were developed that employ the non-linear Full Newton power flow model, optimal power flow, continuation method, or combinations of these approaches [2], [4], [6], [16]. Reference [17] introduces a new security limit within the SSR framework, associated with intermittent generation sources, such as wind farms, to enhance the overall security assessment.

Methods utilizing optimization models to determine steady-state security regions have also been developed. In [10], a linear power flow model and linear programming are employed. The methodology considers only active power limits, which simplifies the calculation but overlooks additional constraints that could influence system security in real-world scenarios.

Methodologies that combine power flow methods and artificial intelligence, such as Fuzzy logic [18], Particle Swarm Optimization (PSO) [11], [19], and neural networks [20] have also been developed. In [21], security limits are determined using neural networks. Three limits are defined: line thermal overload, transformer overload, and voltage instability. The references [22], [23] present a review of the research efforts and the AI-based techniques proposed thus far for DSA, contextualizing and discussing the potential use of artificial intelligence, and interrelating them. The papers also discuss the research opportunities and future trends of AI techniques for security studies.

Recent studies have increasingly focused on the accurate characterization of steady-state security regions in power systems, especially in light of the operational uncertainties introduced by renewable energy sources and integrated energy infrastructures. [24] proposed an efficient method for the accurate identification of critical boundary hyperplanes that define the practical steady-state security region (PSSR) in distribution grids. Their approach significantly reduces the complexity of optimal scheduling problems by identifying only the essential hyperplanes that constrain the PSSR. This yields a compact and generalizable representation of the security region, making the method broadly applicable to a variety of optimization problems, including deliverable energy flexibility scheduling.

In parallel, [25] addressed the SSR in integrated energy systems (IES) by explicitly incorporating thermal dynamics and the coupling effects between power and heating systems. They introduced the concept of the sequential steady-state security region (SSSR) to capture the time-varying nature of the SSR under the influence of combined heat and power (CHP) units and thermal storage dynamics. To solve the SSSR problem, the authors developed an equivalence-based hyperplane method (EHM) that efficiently characterizes the dynamic evolution of security boundaries across multiple time periods. Their findings underscore the importance of accounting for dynamic interactions in ensuring secure and flexible operation of the power system.

Motivation and Contribution of this Work

In the previously referenced works, techniques such as linearization, decoupled methods, and even artificial intelligence have been used to reduce the computational effort in constructing the SSR for power systems. Despite these efforts, reducing computational time remains a significant challenge, especially for real-time or near real-time applications [6], [11]. Based on this, and aiming to improve computational performance in determining security regions, this paper proposes a new methodology using Artificial Neural Networks (ANN) to determine SSR efficiently, reducing investments in the distributed processing environment, focusing primarily on real-time or near real-time applications [6].

The main idea is to define neural networks dedicated to each system loading level within an operational planning environment, enabling their use in real-time or near real-time in a highly efficient manner. Thus, the main contribution of this work is the development of a novel generic methodology based on ANN to determine SSR. The main objective is to reduce the computational time requirements in the SSR construction process compared to traditional methodologies that use power flow. The proposed methodology is tested and validated through the study of two systems, the first one is the 9-Bus tutorial system [26], and the second one is the New England system [27]. The results presented validate and clearly indicate the effectiveness of the proposed technique.

II. Steady-State Security Regions

The Steady-State Security Region represents the region in which the system can operate without violating steady-state limits, such as thermal or voltage constraints [2], [4]. This region is depicted as a three-dimensional graph, enabling a clear visualization of the secure operating region, organized into three generation groups, as shown in Fig. 1. Generator groups are defined according to the objectives of the study, ranging from a single generating unit to sets of plants within a subsystem or from the same river basin, with one group serving as a reference to balance load and generation. The use of three generation groups is commonly observed in the literature [2], [6], [7], [28], providing a balance between model accuracy and computational complexity.

In general, it is advisable to group areas of the power system where monitoring of inter-area power exchanges is needed, along with the assessment of maximum and minimum active power transfer capabilities. These areas require close

monitoring of network nodes and transmission components to define voltage security limits, thereby helping to prevent voltage instability, insufficient reactive power support, and thermal overloading of circuits. Tools like this are particularly valuable for identifying generation transfer limits and supporting secure system operation.

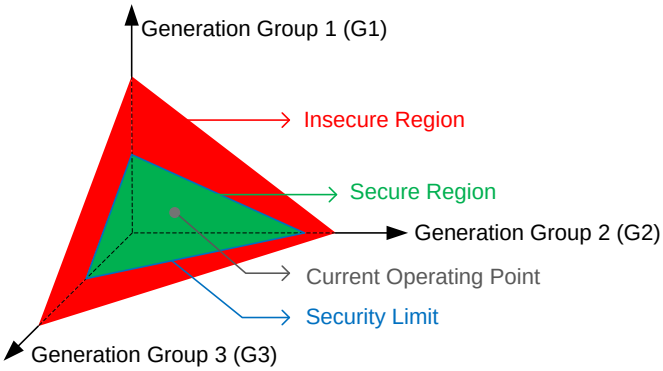

Fig. 1. Generic structure of a SSR for three generations groups, containing the secure region (green), the insecure region (red), operational boundaries and the operating point.

The security region, shown in green in the Fig. 1, is bounded by a frontier beyond which one or more steady-state security limits are violated. These limits include, but are not limited to, bus voltage constraints, reactive power generation limits for generators and synchronous compensators, and thermal capacity limits of transmission lines and transformers.

It is important to note that, as illustrated in Fig. 1, the SSR depicts the system's security boundaries, which are automatically determined by varying generation scenarios to meet a fixed demand while evaluating specific security criteria. The resulting three-dimensional surface is often visualized through nomograms corresponding to its component planes. In [16], the use of such nomograms in voltage security assessments of power systems is demonstrated. For example, Fig. 2 presents the G2–G3 plane, obtained by projecting the three-dimensional SSR from Fig. 1. This representation supports a wide range of applications, including offline studies for expansion planning and system operation, as well as real-time or near real-time use in supervision and control centers [2], [3], [6]. A comprehensive description of the SSR construction process can be found in [4].

III. Proposed Methodology

To reduce the high computational cost associated with the conventional SSR construction approach (summarized in Section I), the methodology proposed in this work uses artificial neural networks to determine the boundaries of the Static Security Regions. The proposed methodology consists of determining five neural networks, with each neural network representing a specific limit of the security region: active power limit, voltage limit, reactive power limit, thermal limit, and security limit [4]. The division of neural networks was chosen because each limit has eight coordinates per generator group in the electrical system. This could complicate the

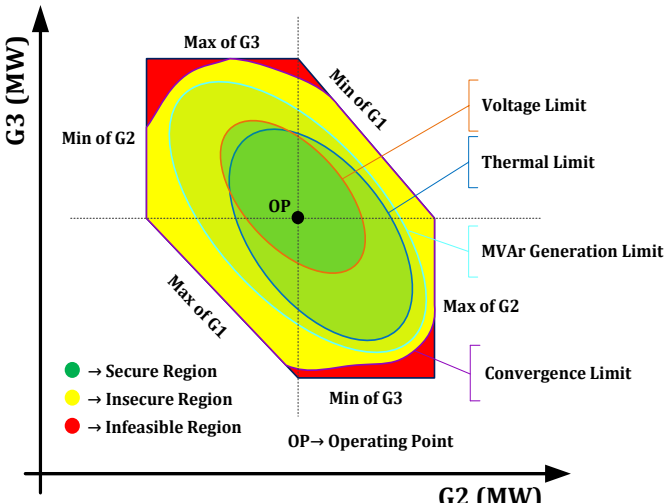

Fig. 2. Typical nomogram for generator groups G2–G3 projected from the three-dimensional SSR surface.

training process if all limits were considered within a single neural network.

The proposed methodology is organized into three distinct environments, as illustrated in Fig. 3: daily operation planning, real-time, and near real-time. In the daily operation planning stage, neural networks are defined and trained using the planned system conditions. This stage is the central component of the methodology. The real-time environment is responsible for monitoring and representing the actual state of the power system. It consists of four key processes: SCADA (Supervisory Control and Data Acquisition), disturbance records, the state estimator, and the system model. The near real-time environment uses the trained neural networks to assess the system at regular intervals—such as every 5 minutes—providing fast and accurate decision support based on the current operating conditions.

The following sections describe each step of the daily operation planning procedure in detail.

A. Data Processing

The neural networks are trained using the coordinates of the security region limits, obtained from a load curve forecasting process. In short-term operation planning, load and generation forecasting is a crucial task and is typically well-developed in the procedures of operating companies. In this work, these coordinates are obtained through an academic version of the production-grade power flow software, ANAREDE, developed by CEPEL (Brazilian Electric Energy Research Center). In ANAREDE, the SSRs are constructed using the conventional method described by [4].

To obtain the SSR limits for training the neural networks, the system load was changed, starting from 70% to 100% of the nominal load, keeping the power factor fixed. Each neural network, representing one of the SSR limits, is trained separately with the obtained data. Five distinct equipment or operational limits (security criteria) are used, which are [4]:

- Reactive power generation limits – "Reactive Power"
- Active power generation group limit – "Active Power"

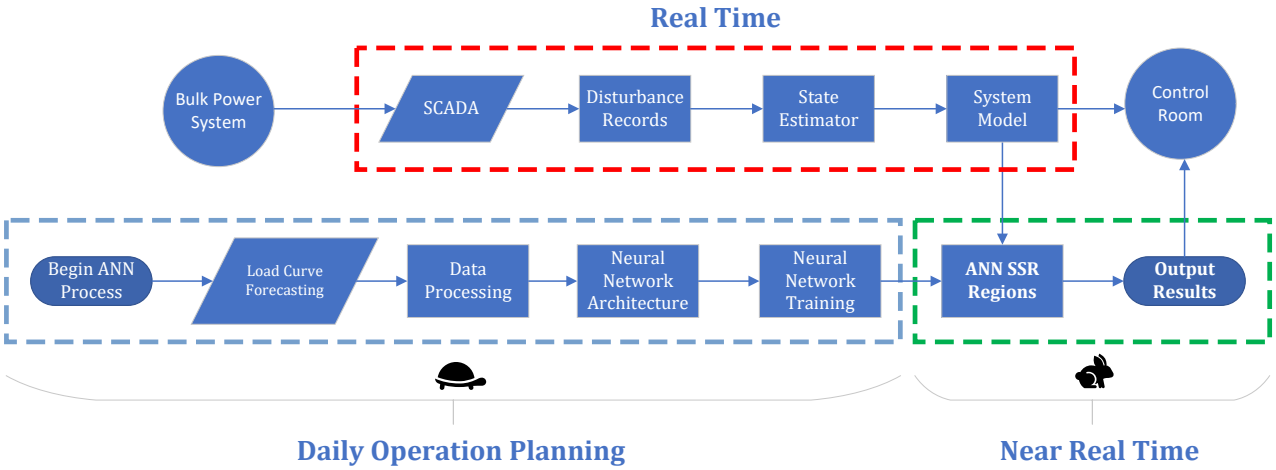

Fig. 3. Flowchart of the proposed methodology, divided into daily operation planning, real-time monitoring, and near real-time application.

- Voltage magnitude limits in all buses – "Voltage"
- Thermal limits in series components – "Thermal"
- Maximum active power transfer – "Security"

For each loading level, a Python-based automation script edits the ANAREDE input files to update the active and reactive load levels proportionally across the system. ANAREDE is then executed, and the resulting output files are parsed. The script extracts the input variables — namely, the active power generated by each generator group and the total active and reactive load of the system — and the corresponding output variables, which consist of boundaries of the security region. These input-output pairs are stored in structured Excel spreadsheets for use in training the neural networks.

The input and output data were normalized by dividing each value by the total active power load of the system. Although this is not a standard Min-Max normalization, it results in values within the range [0,1], since all original values are non-negative and do not exceed the total system load. This per-unit (pu) normalization is commonly used in power system studies, promoting comparability and simplifying the modeling process.

B. Neural Network Architecture

In the proposed methodology, Multilayer Perceptron (MLP) Neural Networks are used through supervised training using the backpropagation algorithm. The number of neurons in the input layer (n_{il}) of each neural network developed is equal to the number of variables in the input set (active power generated by each generator group and total active and reactive loads of the system). Thus, $n_{il} = n_{gg} + 2$, where n_{gg} is the number of generator groups. The number of neurons in the output layer is $n_{ol} = 8 \times n_{gg}$, where each neuron corresponds to one of the eight coordinates of the security region for each generator group in the system. The maximum number of neurons per hidden layer (n_{hl}) is defined according to [29] and is presented in (1):

$$n_{hl} = \frac{2}{3} n_{il} + n_{ol} \tag{1}$$

Each developed MLP neural network is responsible for estimating one of the five limits that make up the security region of the power grid. The decision on whether each neural network will have one or two hidden layers and how many neurons in each layer is made through a Bayesian search [30], using the MATLAB function *bayesopt*. The Bayesian optimization process will perform 50 evaluations to find the best architecture for each neural network, the one with the lowest Mean Squared Error (MSE). The hyperparameters optimized and their respective search intervals were:

- Number of neurons in the first hidden layer: integer in the range $[1, n_{hl}]$;
- Number of neurons in the second hidden layer: integer in the range $[1, n_{hl}]$;
- Number of hidden layers: integer in the range $[1, 2]$.

The objective function used in the Bayesian optimization is the Mean Squared Error (MSE) between the predicted outputs and the actual targets, both normalized by the system base. For each candidate architecture proposed by the Bayesian search, a feedforward neural network is trained and evaluated, and the resulting MSE is used to guide the optimization process. This procedure allows an efficient exploration of the architectural space, leading to high-performance models with minimal manual intervention.

C. Neural Network Training

After defining the architecture, the neural networks were trained using the Deep Learning Toolbox from MATLAB. The weights and biases for the hidden layers were randomly initialized by the toolbox, following its default initialization strategy [31]. The training process used the backpropagation algorithm, optimized using the Levenberg-Marquardt (LM) method. Previous studies have shown that the Levenberg-Marquardt algorithm often provides superior convergence speed and lower training error when compared to standard backpropagation or conjugate gradient methods, especially in small to medium-sized feedforward networks [31]–[33].

The maximum number of epochs was set at 1000, and the maximum number of consecutive validations without improvement before stopping the training (validation checks) was defined as 10. The activation functions used were the hyperbolic tangent for hidden layers and a linear function for

the output layer, both being the default settings of the Deep Learning Toolbox [31].

The LM method dynamically adjusts the update step using a damping factor (μ), which interpolates between the gradient descent and the Gauss-Newton methods. This adaptability eliminates the need for a predefined learning rate, as the method self-regulates its step size based on the training error [34]. This reduces the number of hyperparameters to be tuned during optimization and simplifies the modeling process, without compromising performance. Specifically, when the training error decreases, μ is reduced, making the update step larger and accelerating convergence. In contrast, when the error increases, μ increases, leading to smaller update steps and improving stability.

The training concludes when the gradient norm reaches 10^{-6}, a threshold chosen to ensure stability and convergence while preventing oscillations or divergence in weight updates [35].

To ensure a more reliable evaluation of the developed neural networks, k-fold cross-validation was used during training, with $k = 10$. The choice of $k = 10$ follows recommendations in the literature [36], [37], as it offers a good trade-off between bias and variance in error estimation while keeping computational costs reasonable. The dataset was randomly partitioned into 10 equal subsets. In each iteration, the model was trained on $k - 1$ subsets and validated on the remaining subset. This process was repeated k times, ensuring that each subset was used for both training and validation. The MSE was used to assess the model's performance in each fold. At the end of the process, the network configuration that achieved the lowest average MSE across the folds was selected as the best architecture. This approach reduces the likelihood of overfitting and provides a more robust estimate of the model's generalizability [38].

IV. Results

To validate the proposed methodology, the IEEE 9-Bus tutorial system and the New England test system were employed. In order to emulate typical system operation, an hourly load curve—shown in Fig. 4—was developed based on historical daily demand data from the Brazilian National System Operator (ONS - Brazilian ISO) for the National Interconnected System (SIN). The load curve for November 13, 2023, was selected as a reference, as this date corresponds to one of the historical peak demand records for the SIN.

A. 9-Bus Tutorial System

The IEEE 9-Bus tutorial system is presented in Fig. 5. The system has 3 generators, located at buses 1, 2, and 3, with bus 1 being the system slack bus. The system parameters can be obtained from [26]. Since the system has only three generators, each generator represents a generation group that determines the security regions.

1) Neural Network Architecture: The architectures obtained for each neural network for the 9-Bus tutorial system, along with the limits that define the security region through Bayesian search, are presented in Table I. Since there are three generator groups in the system ($n_{gg} = 3$), the number of neurons in the input layer (n_{il}) of each neural network is 5. The number of neurons in the output layer is $n_{ol} = 24$. Thus, the maximum number of neurons per hidden layer (n_{hl}) according to Equation 1, is 28. The Bayesian search determined that each neural network will have two hidden layers.

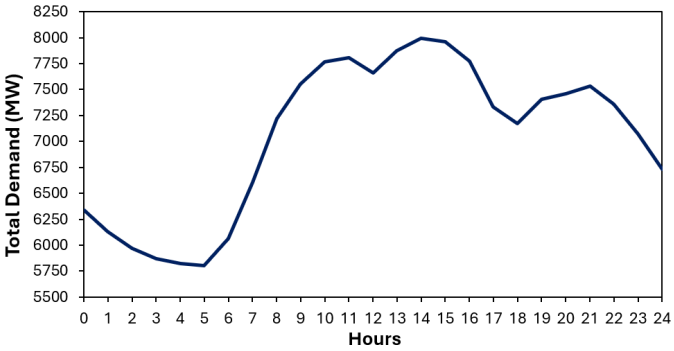

Fig. 4. Load curve with load levels for the IEEE 9-Bus tutorial system.

TABLE I
ARCHITECTURES OBTAINED FOR NEURAL NETWORKS – 9-BUS TUTORIAL SYSTEM

SSR Limits	Layer 1	Layer 2	MSE
Reactive Power	17	27	2.41×10^{-9}
Active Power	25	28	3.03×10^{-9}
Voltage	22	12	3.47×10^{-8}
Thermal	22	4	6.6×10^{-9}
Security	20	17	3.29×10^{-9}

2) Neural Network Training: The nominal load of the 9-Bus Tutorial System, 315 MW, and 115 MVAr, was reduced by up to 30% at all load buses while keeping the power factor constant. The generation specified at the PV buses was also adjusted according to the system loading percentage. Subsequently, the coordinates of the security region limits for training the neural networks were obtained using ANAREDE software, as described in Subsection III-C. During neural network training, *k-fold* cross-validation was used, and the neural network with the lowest MSE was chosen for each security region limit, as shown in Table II.

TABLE II
CROSS-VALIDATION TRAINING RESULTS FOR THE 9-BUS SYSTEM

SSR Limits	Average MSE	SD MSE	Lower MSE
Reactive power	6.70×10^{-8}	5.56×10^{-8}	5.30×10^{-9}
Active power	4.87×10^{-8}	3.41×10^{-8}	1.74×10^{-8}
Voltage	1.98×10^{-7}	1.94×10^{-7}	4.24×10^{-8}
Thermal	1.05×10^{-7}	2.12×10^{-7}	1.08×10^{-8}
Security	6.35×10^{-8}	7.82×10^{-8}	7.58×10^{-9}

3) SSR for 9-Bus Tutorial System: After training, the data from the load curve shown in the Fig. 4 is applied to the neural networks and thus determines the security regions. The ANAREDE program was used to compare the results obtained by the proposed methodology with the conventional methodology for constructing SSRs [4].

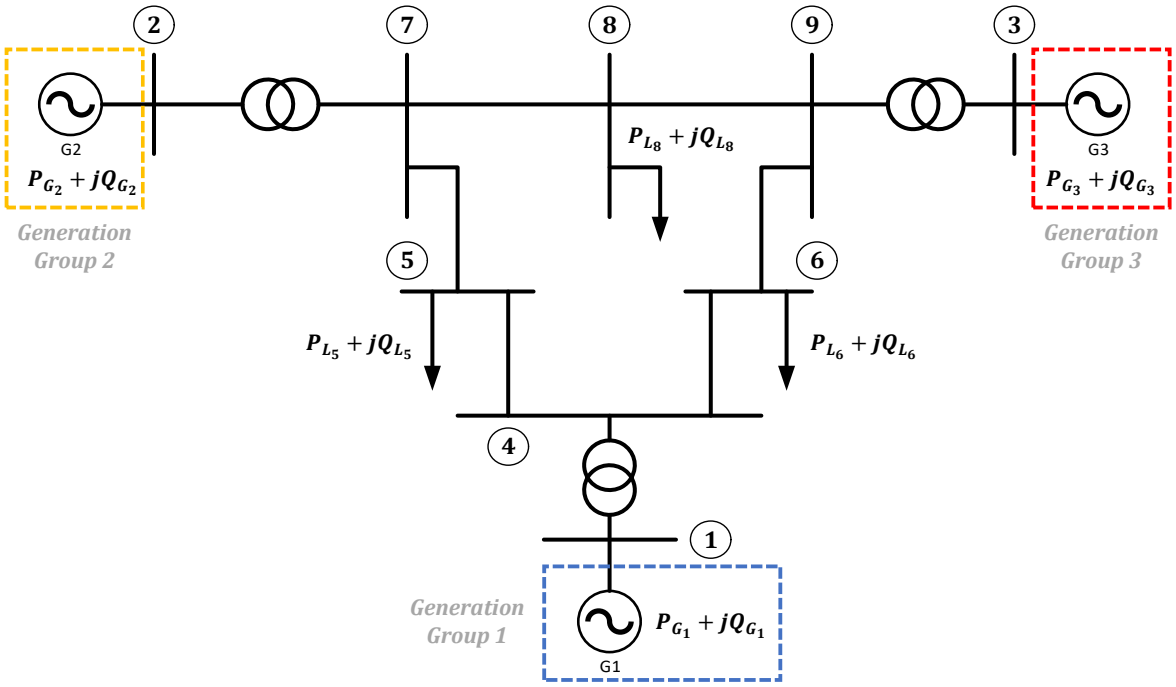

Fig. 5. Topology and generation groups for 9-Bus tutorial system.

The highest errors obtained for each neural network considering all hourly intervals of the load curve are shown in Table III. For each security region limit, the mean squared errors between the actual limits obtained by the ANAREDE software and the limits estimated by the neural networks are presented. The errors are calculated both with the normalized neural network outputs and with the outputs converted to MW. Additionally, Table III presents the highest absolute errors for each limit that composes the security region and the time of the load curve where the errors were obtained.

Table III shows that, when comparing the coordinates of the SSR limits obtained by ANAREDE and the proposed methodology, the 9-Bus tutorial system operating at 8 pm presented the largest absolute errors in MW in three of the five limits. At 8 pm, the 9-Bus tutorial system has an active load of 293.89 MW, corresponding to 93.3% of the system's nominal load, 315 MW.

Figs. 6 and 7 present the security region obtained through the proposed methodology and ANAREDE program, for the 9-Bus system operating at 8:00 pm. Only the G2xG3 plane will be presented due to a lack of space. In Fig. 6, each security region limit is represented by a different color, and as they overlap, they form the system's security region, shown in dark green at the center. The figure also shows the system's operating point (OP), which represents the generation needed to meet the system's current load.

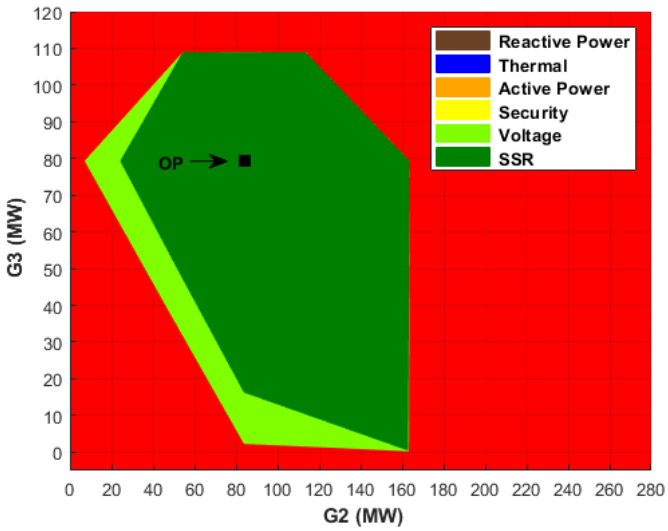

Fig. 6. SSR obtained by the proposed methodology for the 9-Bus system operating at 8:00 pm.

B. New England System

The New England 39-Bus, 10-machine system is used to validate the proposed methodology. Fig. 8 shows the system topology and the indication of the three generator groups. The system parameters can be obtained from [27].

1) Neural Network Architecture: Table IV presents the architectures obtained for each neural network, together with the limits that define the safety region through the Bayesian search. Since the number of generator groups in this system is also equal to three ($n_{gg} = 3$), as in the 9-Bus tutorial system, the neural network parameters remain unchanged. Thus, each network has $n_{il} = 5$ neurons in the input layer and $n_{ol} = 24$ in the output layer. According to Equation 1, the maximum

TABLE III
RESULTS OBTAINED FOR THE 9-BUS SYSTEM CONSIDERING LOAD CURVE IN COMPARISON WITH ANAREDE

SSR Limits	MSE	MSE (MW)	Abs. Error	Abs. Error (MW)	Hour
Reactive power	1.07×10^{-8}	0.0011	0.0011	0.3548	10 pm
Active power	4.87×10^{-8}	0.0048	0.0019	0.5915	8 pm
Voltage	1.84×10^{-7}	0.0183	0.0058	1.8149	1 pm
Thermal	2.57×10^{-8}	0.0026	0.0018	0.5620	8 pm
Security	1.15×10^{-8}	0.0011	0.0010	0.3230	8 pm

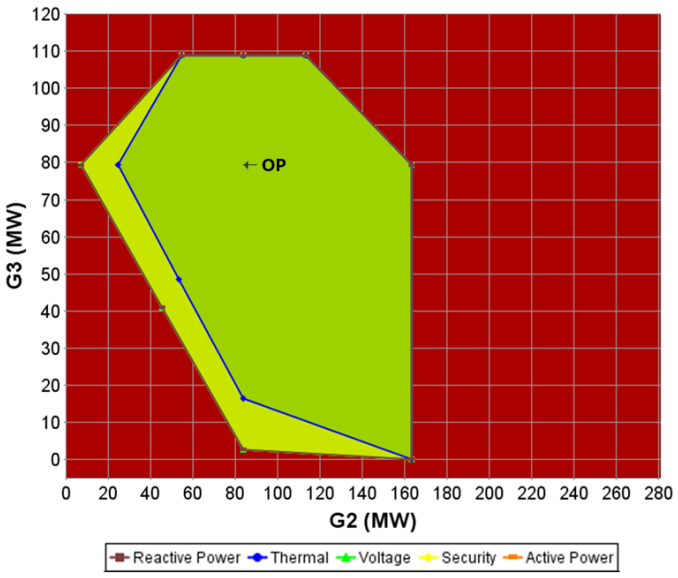

Fig. 7. SSR obtained by the ANAREDE for the 9-Bus system operating at 8:00 pm.

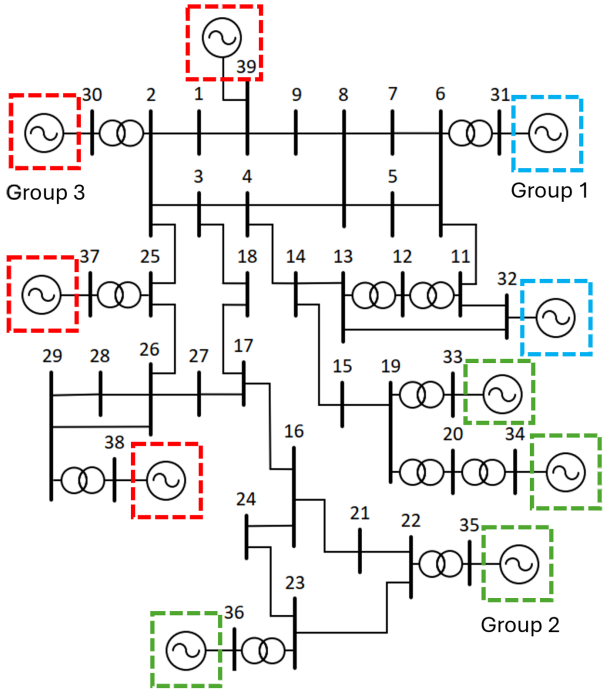

Fig. 8. Topology and generator groups for the New England system.

number of neurons per hidden layer (n_{hl}) is 28. The Bayesian search defined an architecture with two hidden layers for each network.

TABLE IV
ARCHITECTURES OBTAINED FOR NEURAL NETWORKS – NEW ENGLAND SYSTEM

SSR Limits	Layer 1	Layer 2	MSE
Reactive Power	21	17	4.50×10^{-9}
Active Power	24	28	3.27×10^{-9}
Voltage	13	11	2.30×10^{-9}
Thermal	18	25	3.18×10^{-9}
Security	26	18	2.65×10^{-9}

2) Neural Network Training: After determining the neural network architecture to determine the SSR, the neural networks were trained. The training process is the same as that adopted for the 9-Bus system. Keeping the power factor constant, the nominal load of the New England system, 7,995.5 MW and 1,831.45 MVAr, was reduced by up to 30% in all load buses. The ANAREDE software was used to obtain the coordinates of the limits that make up the safety region for training. The generation specified in the PV buses was also adjusted according to the system load percentage. During the training stage of the neural networks, *k-fold* cross-validation was used, and the neural network with the lowest MSE was chosen for each boundary of the safety region, as shown in Table V.

TABLE V
CROSS-VALIDATION TRAINING RESULTS FOR THE NEW ENGLAND SYSTEM

SSR Limits	Average MSE	SD MSE	Lower MSE
Reactive power	3.31×10^{-8}	3.02×10^{-8}	7.57×10^{-9}
Active power	6.02×10^{-8}	3.71×10^{-8}	1.41×10^{-8}
Voltage	6.30×10^{-8}	3.41×10^{-8}	1.50×10^{-8}
Thermal	1.26×10^{-8}	6.70×10^{-9}	4.30×10^{-9}
Security	3.39×10^{-8}	4.10×10^{-8}	2.10×10^{-9}

3) SSR for New England System: The data from the load curve presented in Fig. 4 are applied to the trained neural networks and thus determine the safety regions. Considering all hourly intervals of the load curve for the New England system, the highest errors obtained for each neural network in the estimation of the safety region compared with the ANAREDE program are shown in Table VI. Figs. 9 and 10 present the security region obtained through the proposed methodology and ANAREDE, for the New England system operating at 6 am, a time that presented the largest absolute error in MW, considering the voltage limit, according to Table VI.

TABLE VI
RESULTS OBTAINED FOR THE NEW ENGLAND SYSTEM CONSIDERING LOAD CURVE IN COMPARISON WITH ANAREDE

SSR Limits	MSE	MSE (MW)	Abs. Error	Error (MW)	Hour
Reactive power	6.57×10^{-9}	0.4207	0.0006	4.6550	6 pm
Active power	1.09×10^{-8}	0.6967	0.0007	5.5894	1 am
Voltage	1.22×10^{-8}	0.7811	0.0010	8.3373	6 am
Thermal	3.67×10^{-9}	0.2348	0.0004	3.0584	2 pm
Security	5.50×10^{-9}	0.3523	0.0006	5.0380	5 pm

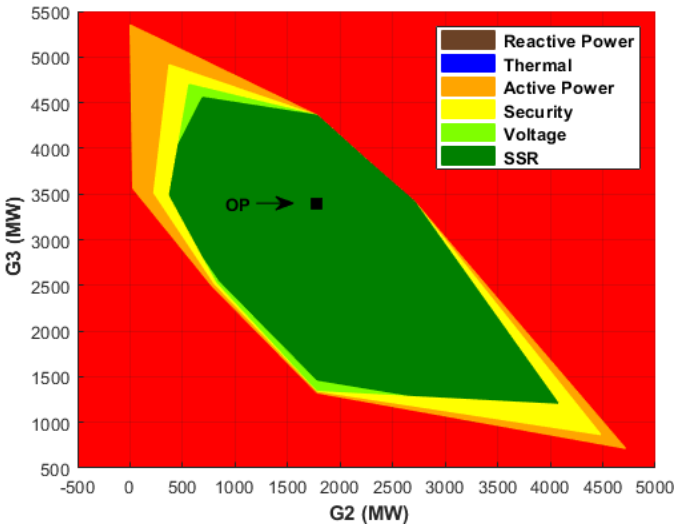

Fig. 9. SSR obtained by the proposed methodology for the New England system operating at 6:00 am.

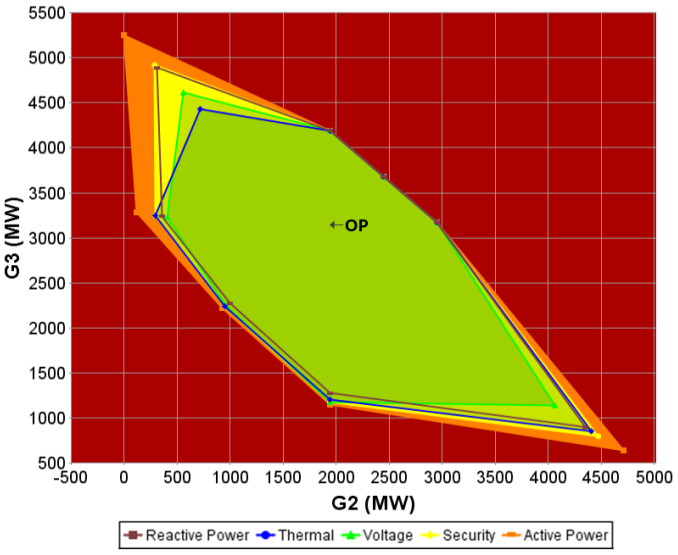

Fig. 10. SSR obtained by the ANAREDE for the New England system operating at 6:00 am.

C. Computational Performace

The neural network training and simulations with load curves were performed on a computer with an Intel CORE i7 processor, 8th generation, 1.99 GHz processor, and 12 GB of RAM. Table VII compares the average computational times obtained by the ANAREDE program and the proposed methodology in determining the security regions for the 9-Bus and the 39-Bus New England systems.

The offline process — comprising the architecture definition and neural network training steps — took 1841.7 s for the IEEE 9-Bus system and 3022.1 s for the New England system. These steps are executed only once for each system, but their computational times were accounted for in the system load conditions analyzed in Section IV. The online process — in which the SSR is obtained using the neural networks trained in the offline — took 4.2 s for the IEEE 9-Bus system and 4.4 s for the New England system.

The computational gain in the "online" step, comparing the proposed methodology with ANAREDE, is quite significant, as seen in Table VII. Although the offline step can be time-consuming, once the neural networks are trained, the limits of the security regions can be determined almost instantly.

For the New England system, the proposed methodology achieved a computational time reduction of 96.05% compared to the conventional SSR construction method. This gain surpasses the 52.42% reduction reported in [11], which employs a PSO-based approach to determine the SSRs. This result underscores the effectiveness of using neural networks as surrogate models to accelerate the construction of static security regions.

D. Discussion and Future Work

The results obtained for the 9-Bus system and the 39-Bus New England systems demonstrate that the developed methodology is accurate in determining the SSR. Due to a lack of space, it was not possible to outline the SSR graphs for all load curve. Compared to ANAREDE, for any loading level and security region limit, the mean squared errors are small, even when calculated in MW after the security region estimations. Although the largest absolute error obtained of 8.3373 MW for the New England system may seem significant, it is important to point out that the system load is around 8,000 MW, which reduces the impact of this error (less than 0.2%). For the 9-Bus tutorial system, the largest absolute error in MW, 1.8149, is only 0.6% of the total system load, 315 MW. Moreover, this limitation is highly compensated by the exceptional computational performance achieved, as demonstrated in the comparison presented in the Subsection IV-C. It is also worth noting that the nomograms obtained by the proposed methodology and by ANAREDE are practically identical, with differences that are only noticeable through the quantitative error analysis.

As the proposed methodology achieves high precision and significant computational gains, some limitations must still be highlighted. Firstly, only artificial neural networks have been investigated as substitute models for conventional SSR

TABLE VII
COMPUTATIONAL PERFORMANCE BETWEEN ANAREDE AND THE PROPOSED METHODOLOGY

System	ANAREDE	Proposed Methodology		Gain (Online Process) (%)
		Offline Process	Online Process	
9-Bus	92.0 s	1841.7 s	4.2 s	**95.43**
New England	111.5 s	3022.1 s	4.4 s	**96.05**

construction techniques. Future studies can explore and compare the performance of the proposed methodology with other artificial intelligence techniques. Also, the precision of the model depends strongly on the quality and representativeness of the training data, and their performance may be prejudiced in poorly represented scenarios during the training. The current model also does not quantify uncertainties, providing only point estimates of the limits of the security region. The incorporation of probabilistic outputs and the adaptation of the approach to dynamic operating conditions or larger energy systems represent promising directions for future research. Since this study uses the Mean Squared Error (MSE) and the absolute error as performance metrics, other measures could complement the evaluation of the quality of the model.

Another limitation of the proposed method is the long computational time necessary in the offline phase, particularly for the definition of the architecture and the training of neural networks. If each limit that makes up the SSR contains more than eight coordinates per generator group, the resulting representation is more detailed, but requires even greater computational effort. It is also worth highlighting that all stages of the proposed methodology are only executed sequentially, which further increases the offline time. The total offline process includes the time spent on Bayesian optimization and no training for each of the SSR limits. In future research, we intend to explore the use of parallel computing to reduce computational costs, especially in applications related to Dynamic Security Assessment (DSA), as discussed in [3], [6].

V. CONCLUSION

This paper described a new methodology to determine Steady-State Security Regions accurately and efficiently. The proposed methodology is based on artificial neural networks to determine the secure limits of the system, considering each load level. The 9-Bus tutorial system and the New England systema validated the proposed methodology. After training the neural networks, the validation of the methodology was performed considering an hourly load curve in the operations of the test systems.

From the results, it is observed that the security regions of the test systems change according to the system loading level, and electrical system operators must have a fast and accurate tool to determine these regions. The proposed methodology proved to be efficient and effective in meeting the computational speed required, with precision in determining the security regions, and can be a useful tool for operating electrical systems, especially in real-time and near real-time or analyses when the evaluation of a large number of scenarios is required. The proposed methodology will be expanded to analyze dynamic security regions in future research work.

ACKNOWLEDGMENTS

The authors would like to thank the Brazilian Federal Agency for Support and Evaluation of Graduate Education (CAPES), the National Research Council (CNPq), and the State of Minas Gerais Research Foundation (FAPEMIG). They also thank UFJF, and CEFET/RJ.

REFERENCES

[1] T. Adefarati and R. Bansal, "Integration of renewable distributed generators into the distribution system: a review," *IET Renewable Power Generation*, vol. 10, no. 7, pp. 873–884, 2016. doi: https://doi.org/10.1049/iet-rpg.2015.0378 .

[2] K. Morison, L. Wang, and P. Kundur, "Power system security assessment," *IEEE Power and Energy Magazine*, vol. 2, no. 5, pp. 30–39, 2004. doi: 10.1109/MPAE.2004.1338120 .

[3] K. Morison, "On-line dynamic security assessment using intelligent systems," in *2006 IEEE Power Engineering Society General Meeting*, 2006, pp. 5 pp.–. doi: 10.1109/PES.2006.1709501 .

[4] F. C. Almeida, J. A. P. Filho, J. L. Pereira, R. M. Henriques, and A. L. Marcato, "Assessment of load modeling in power system security analysis based on static security regions," *Journal of Control, Automation and Electrical Systems*, vol. 24, pp. 148–161, 4 2013. doi: 10.1007/s40313-013-0020-7 .

[5] R. Diao, V. Vittal, and N. Logic, "Design of a real-time security assessment tool for situational awareness enhancement in modern power systems," *IEEE Transactions on Power Systems*, vol. 25, no. 2, pp. 957–965, 2010. doi: 10.1109/TPWRS.2009.2035507 .

[6] S. C. Savulescu, *Real-time stability assessment in modern power system control centers*. USA: John Wiley & Sons, 2009.

[7] C. A. S. Neto, M. A. Quadros, M. G. Santos, and J. Jardim, "Brazilian system operator online security assessment system," in *IEEE PES General Meeting*, 2010, pp. 1–7. doi: 10.1109/PES.2010.5590039 .

[8] O. F. Avila, J. A. Passos Filho, and W. Peres, "Steady-state security assessment in distribution systems with high penetration of distributed energy resources," *Electric Power Systems Research*, vol. 201, p. 107500, 2021. doi: https://doi.org/10.1016/j.epsr.2021.107500 .

[9] J. Xiao, S. Zhang, Z. Qiu, C. Song, H. Jiao, and B. She, "Geometric property of distribution system security region: Size and shape," *Electric Power Systems Research*, vol. 210, p. 108106, 2022. doi: 10.1016/j.epsr.2022.108106 .

[10] J. Zhu, R. Fan, G. Xu, and C. Chang, "Construction of maximal steady-state security regions of power systems using optimization method," *Electric Power Systems Research*, vol. 44, no. 2, pp. 101–105, 1998. doi: 10.1016/S0378-7796(97)01188-7 .

[11] R. A. G. Tinoco, J. A. Passos Filho, W. Peres, and R. M. Henriques, "A new particle swarm optimization-based methodology for determining online static security regions," *International Transactions on Electrical Energy Systems*, vol. 31, no. 3, p. e12790, 2021. doi: https://doi.org/10.1002/2050-7038.12790 .

[12] C.-C. Liu, "A new method for the construction of maximal steady-state security regions of power systems," *IEEE Transactions on Power Systems*, vol. 1, no. 4, pp. 19–26, 1986. doi: 10.1109/TPWRS.1986.4335009 .

[13] S. J. Chen, Q. X. Chen, Q. Xia, and C. Q. Kang, "Steady-state security assessment method based on distance to security region boundaries," *IET Generation, Transmission & Distribution*, vol. 7, no. 3, pp. 288–297, 2013. doi: 10.1049/iet-gtd.2012.0288 .

[14] F. Wu and S. Kumagai, "Steady-state security regions of power systems," *IEEE Transactions on Circuits and Systems*, vol. 29, no. 11, pp. 703–711, 1982. doi: 10.1109/TCS.1982.1085091 .

[15] F. Wu, Y.-K. Tsai, and Y.-X. Yu, "Probabilistic steady-state and dynamic security assessment," *IEEE Transactions on Power Systems*, vol. 3, no. 1, pp. 1–9, 1988. doi: 10.1109/59.43173 .

[16] H. Sarmiento, G. Pampin, R. Barajas, R. Castellanos, G. Villa, and M. Mirabal, "Nomograms for assistance in voltage security visualization," in *2009 IEEE/PES Power Systems Conference and Exposition*, 2009, pp. 1–6. doi: 10.1109/PSCE.2009.4840049 .

[17] F. M. Tavela, J. A. Filho, and O. F. Avila, "Assessment of the impact of wind generation intermittency on electric power systems through security regions," *Journal of Control, Automation and Electrical Systems*, vol. 33, pp. 982–997, 6 2022. doi: 10.1007/S40313-021-00870-2 .

[18] H. Sun, D. Yu, and Y. Xie, "Flexible steady-state security region of power system with uncertain load demand and soft security limits," in *2000 Power Engineering Society Summer Meeting (Cat. No.00CH37134)*, vol. 4, 2000, pp. 2008–2013 vol. 4. doi: 10.1109/PESS.2000.866955 .

[19] S. Maihemuti, W. Wang, J. Wu, H. Wang, M. Muhedaner, and Q. Zhu, "New energy power system dynamic security and stability region calculation based on avurpso-rls hybrid algorithm," *Processes*, vol. 11, no. 4, 2023. doi: 10.3390/pr11041269 .

[20] Y. Yu, "Security region of bulk power system," in *Proceedings. International Conference on Power System Technology*, vol. 1, 2002, pp. 13–17 vol.1. doi: 10.1109/ICPST.2002.1053495 .

[21] J. D. McCalley, G. Zhou, and V. V. Acker, "Power system security boundary visualization using neural networks," *Neurocomputing*, vol. 23, no. 1, pp. 85–96, 1998. doi: https://doi.org/10.1016/S0925-2312(98)00077-0 .

[22] J. Jardim, "Online dynamic security assessment: implementation problems and potential use of artificial intelligence," in *Power Engineering Society Summer Meeting*, vol. 1, 2000, pp. 340–345. doi: 10.1109/PESS.2000.867607 .

[23] M. Cuevas, R. Álvarez Malebrán, C. Rahmann, D. Ortiz, J. Peña, and R. Rozas-Valderrama, "Artificial intelligence techniques for dynamic security assessments - a survey," *Artificial Intelligence Review 2024 57:12*, vol. 57, pp. 1–43, 10 2024. doi: 10.1007/S10462-024-10993-Y .

[24] D. Sun and Y. Yu, "Accurate identification of critical boundary hyperplanes of practical steady-state security region in distribution grids," *IEEE Transactions on Smart Grid*, vol. 14, no. 6, pp. 4312–4321, 2023. doi=10.1109/TSG.2023.3262693. doi: 10.1109/TSG.2023.3262693 .

[25] S. Zhang, W. Gu, X.-P. Zhang, H. Lu, S. Lu, S. Ding, J. Wang, and S. Zhao, "Steady-state security region of integrated energy system considering thermal dynamics," *IEEE Transactions on Power Systems*, vol. 39, no. 2, pp. 4138–4153, 2024. doi: 10.1109/TPWRS.2023.3296080 .

[26] P. M. Anderson and A. A. Fouad, *Power system control and stability*. John Wiley & Sons, 2008.

[27] G. Bills, "On-line stability analysis study, rp 90-1," North American Rockwell Information Systems Co., Anaheim, CA (USA), Tech. Rep., 1970.

[28] F. C. B. Almeida, J. A. P. Filho, J. L. R. Pereira, A. L. M. Marcato, and E. J. de Oliveira, "Assessment of the generator remote voltage control through static security regions," in *2011 IEEE Power and Energy Society General Meeting*, 2011, pp. 1–7. doi: 10.1109/PES.2011.6039630 .

[29] J. Heaton, *Introduction to Neural Networks with Java*. Saint Louis: Heaton Research, 2008.

[30] N. Friedman and D. Koller, "Being bayesian about network structure. a bayesian approach to structure discovery in bayesian networks," *Machine learning*, vol. 50, pp. 95–125, 2003. doi: 10.1023/A:1020249912095 .

[31] M. H. Beale, M. T. Hagan, and H. B. Demuth, *Deep Learning Toolbox User's Guide*. Natick: The MathWorks, 2018.

[32] M. Hagan and M. Menhaj, "Training feedforward networks with the marquardt algorithm," *IEEE Transactions on Neural Networks*, vol. 5, no. 6, pp. 989–993, 1994. doi: 10.1109/72.329697 .

[33] I. A. Basheer and M. Hajmeer, "Artificial neural networks: fundamentals, computing, design, and application," *Journal of microbiological methods*, vol. 43, no. 1, pp. 3–31, 2000. doi: 10.1016/S0167-7012(00)00201-3 .

[34] C. Bishop, *Neural networks for pattern recognition*. Clarendon Press, 1995, vol. 2.

[35] R. Battiti, "First- and second-order methods for learning: Between steepest descent and newton's method," *Neural Computation*, vol. 4, no. 2, pp. 141–166, 1992. doi: 10.1162/neco.1992.4.2.141 .

[36] R. Kohavi *et al.*, "A study of cross-validation and bootstrap for accuracy estimation and model selection," in *Ijcai*, vol. 14, no. 2. Montreal, Canada, 1995, pp. 1137–1145. doi: 10.5555/1643031.1643047 .

[37] G. James, D. Witten, T. Hastie, and R. Tibshirani, *An introduction to statistical learning with applications in R*. Springer, 2013.

[38] S. Russell and P. Norvig, *Artificial Intelligence: A Modern Approach*, 3rd ed. Upper Saddle River, NJ: Prentice Hall, 2010.

Guilherme de Oliveira Alves received his B.Sc. (2014), M.Sc. (2015), and D.Sc. (2021) from the Federal University of Juiz de Fora (UFJF). From 2021 to 2022, he worked as a Researcher at the Electrical Sector Study Group (GESEL) of the Federal University of Rio de Janeiro (UFRJ). From 2022 to 2023, he worked at the Department of Electrical Engineering of the Federal University of Juiz de Fora. Since 2024, he has been with the Department of Electrical Engineering of the Federal Center for Technological Education "Celso Suckow da Fonseca" (CEFET/RJ), RJ, Brazil. His main research interests are power grid analysis, optimization, and voltage safety analysis.

João Alberto Passos Filho (M'07–SM'12) received his B.Sc. (1995) and M.Sc. (2000) from the Federal University of Juiz de Fora (UFJF) and D.Sc. (2005) Degree from the Federal University of Rio de Janeiro (COPPE/RFRJ). From 1997 to 2009 he worked at Electric Energy Research Center (CEPEL) on developing power system analysis software. Since 2009, he has been with the Department of Electrical Engineering of the Federal University of Juiz de Fora, MG, Brazil. At UFJF, he served as head of the Department of Electrical Energy for two terms from 2011 to 2015. He also served as the coordinator of the graduate program in Electrical Engineering at UFJF in 2019 and 2020. His main research interests are voltage security analysis, optimization, and control of power systems. Additionally, he has been working as an associate editor for academic journals IEEE Transactions on Sustainable Energy and IEEE Power Engineering Letters.